Atmospheric and Climate Sciences, 2024, 14, 407-428
https://www.scirp.org/journal/acs
ISSN Online: 2160-0422
ISSN Print: 2160-0414

CO_2 Back-Radiation Sensitivity Studies under Laboratory and Field Conditions

Ernst Hammel, Martin Steiner, Christoph Marvan, Matthias Marvan, Klaus Retzlaff, Werner Bergholz, Axel Jacquine

International Climate Research, A Citizen Research Group, Vienna, Austria
Email: ernst@icr2025.org, steiner@icr2025.org

How to cite this paper: Hammel, E., Steiner, M., Marvan, C., Marvan, M., Retzlaff, K., Bergholz, W. and Jacquine, A. (2024) CO_2 Back-Radiation Sensitivity Studies under Laboratory and Field Conditions. *Atmospheric and Climate Sciences*, **14**, 407-428.
https://doi.org/10.4236/acs.2024.144025

Received: July 19, 2024
Accepted: October 6, 2024
Published: October 9, 2024

Abstract

We measured the IR back radiation using a relatively low-cost experimental setup and a test chamber with increasing CO_2 concentrations starting with a pure N_2 atmosphere against a temperature-controlled black reference background. The results confirm estimations within this work and previous finding about CO_2-induced infrared radiation saturation within realistic atmospheric conditions. We used this setup also to study thermal forcing effects with stronger and rare greenhouse gases against a clear night sky. Our results and their interpretation are another indication for having a more critical approach in climate modelling and against monocausal interpretation of climate indices only caused by anthropogenic greenhouse gas emissions. Basic physics combined with measurements and data taken from the literature allow us to conclude that CO_2 induced infrared back-radiation must follow an asymptotic logarithmic-like behavior, which is also widely accepted in the climate-change community. The important question of climate sensitivity by doubling current CO_2 concentrations is estimated to be below 1˚C. This value is important when the United Nations consider climate change as an existential threat and many governments intend rigorously to reduce net greenhouse gas emissions, led by an ambitious European Union inspired by IPCC assessments is targeting for more than 55% in 2030 and up to 100% in 2050 [1]. But probably they should also listen to experts [2] [3] who found that all these predictions have considerable flaws in basic models, data and impact scenarios.

Keywords

Climate Change, Greenhouse Gases, CO_2 Backscatter, IR Radiation

1. Introduction

Our atmosphere mainly comprises radiative inactive diatomic molecules N_2

78.08% and O_2 20.95% by volume. The remaining 0.97% consists primarily in Ar with 0.93%, CO_2 with 0.04% in volume, and traces of hydrogen, helium, and other noble gases, methane, nitrous oxide, and ozone. A variable but radiatively dominant part is water vapor, which is on average about 1% in volume at sea level. Greenhouse (GH) molecules absorb terrestrial IR radiation emitted by the surface as result of warming caused by the incoming solar radiation. Their absorption characteristics allow them to act in the retention of heat within the atmosphere and to ensure that the global mean temperature of the atmosphere supports biological life. This is commonly known as the greenhouse effect. Therefore, the IR active components are water vapor, carbon dioxide, methane, dinitrogen monoxide, and ozone, in decreasing order of effectiveness due to their concentrations.

The infrared IR transmission spectra of CO_2 over a path length of 100 meters is shown in Figure 1 against the wavenumber, $1/\lambda = \nu/c$ (λ = wavelength, ν = frequency, c = velocity of light). The transmission T or transmittance is the extent by which the incident radiation at any wave number is transmitted by the sample. For opaque media T = 0 and complete transparent media T = 1.

In reflection-free media absorbance, A = 1 − T (transmittance) according to Kirchhoff's law, which also allows the propagation of the equality of long wave emissivity ε and absorptivity a_{lw}.

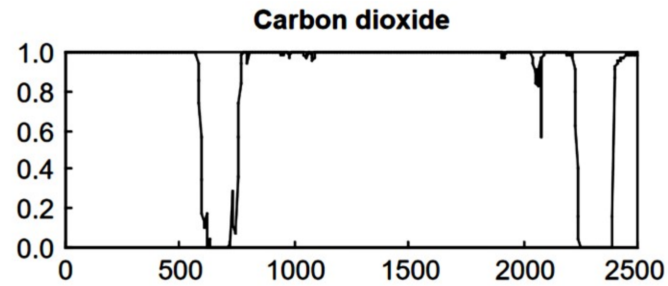

Figure 1. CO_2 IR Transmittance over 100 meters as a function of wavenumber from HITRAN [4].

The CO_2 spectrum is dominated by the bending vibration, centered at 667 cm^{-1} equivalent to a wavelength of 14.992 μm, and the asymmetrical stretching mode at 2349 cm^{-1} equivalent to 4.257 μm. The extra and very weak bands arise from further excitations and represent very small absorptions that are very often claimed to be significantly inaccurate calculations of the GH effect.

The surface has a mean global temperature of 288˚K and its emission is approximated by a black body at this temperature, consisting of a continuous radiation spectrum unlike that of the GH gases which is specific for each molecule-species and made up of discrete rotation-vibrational bands. The continuous Planck or black body surface radiance is shown by the gray curve in Figure 2 compared to the limits of the CO_2 absorption bands in orange and red of the main GH gas of CO_2.

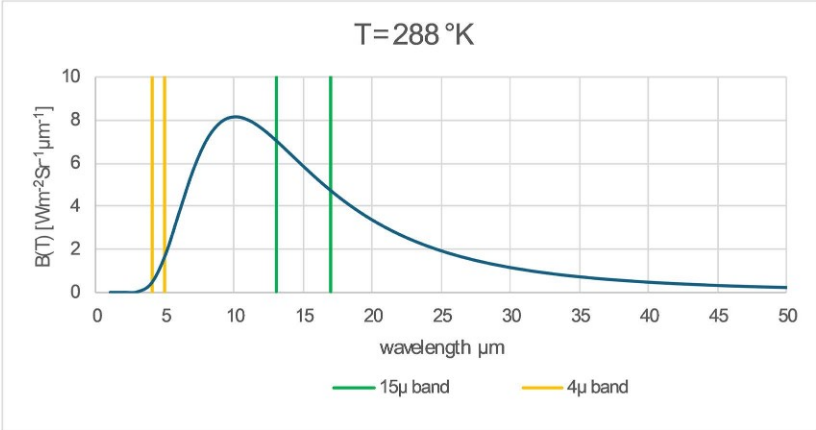

Figure 2. Black body radiator at T = 288˚K and major CO_2 absorption bands.

The contribution of the 15 µm and the 4 µm CO_2 band to the total black body IR absorption can be estimated by integration of Figure 1 with a rough maximum of 25%, where the major contribution comes from the 15 µm band.

The solar irradiance intercepted by our atmosphere is $\pi a^2 S_0$, where a is the earth's radius. A fraction α, called the planetary albedo is reflected to space. The remaining portion is absorbed. Averaging over a long time over the total area of the globe, the absorbed solar radiation must be in balance with the radiation emitted by the atmosphere. In a very simplified 2D model we get according to Stefan-Boltzmann

$$(1-\alpha)\frac{S_0}{4} = \sigma T_E^4 \quad (1)$$

where T_E is the theoretical emission temperature without any atmospheric greenhouse effect. Assuming on average α = 0.3, we find T_E = 255˚K, a temperature much lower than the observed global average surface temperature of T_S = 288˚K. That means that the natural greenhouse effect results in additional ΔT_{GH} = 33˚K, corresponding to

$$\sigma T_S^4 - \sigma T_E^4 = 150\,\mathrm{W/m^2} \quad (2)$$

Detailed evaluation of the Planck function for T_S = 15˚C or 288˚K, results in the respective absorption bands.

13.26 - 17.07 µm (15 µ band), in energy densities of 9.22×10^{-7} J/m³ or 17.6% of the total emission or 6.95×10^{13} photons per m³.

4.19 - 4.38 µm (4 µ band), in energy densities of 5.72×10^{-9} J/m³, being 0.11% of the total emission or 1.22×10^{11} photons per m³.

From above considerations, we see that only the 15 µ band is significant with an IR absorption limited to 0.176 × 391 W/m² = 69 W/m² and back-radiation to 69/2 = 34.5 W/m². Simplified energy balance considerations in a single atmospheric layer are sketched in the following drawing. See Figure 3.

With $\varepsilon = 1$ we get

$$\sigma T_S^4 = U = 2\sigma T_A^4 = 2\sigma T_E^4 \quad (3)$$

and

$$T_S = \sqrt[4]{2} \cdot T_E \tag{4}$$

With T_E = 255˚K we therefore obtain T_S = 303˚K. This value is considerably higher than the observed 288˚K. The discrepancy between theory and observation is explained by the fact that the atmosphere is not totally opaque to long-wave radiation. The presence of the atmosphere raises the temperature at the Earth's surface considerably. It is known that this effect is referred to as the greenhouse effect. We assume now that the atmosphere is semi-grey, *i.e.* it absorbs a constant fraction ε of the long-wave radiation, but is still transparent to solar radiation and emits upwards and downwards at a rate given by

$$B = \varepsilon\sigma T_A^4 = \frac{\varepsilon}{2-\epsilon}\sigma T_E^4 \tag{5}$$

where σT_A^4 is the radiation energy content of atmosphere. This leads to

$$T_S = \sqrt[4]{\frac{2}{2-\epsilon}} \cdot T_E \tag{6}$$

With $\varepsilon = 0.78$, we then obtain $T_S = 288$˚K. We can conclude that in this simplified model only 22% or 42.8 W/m^2 of the IR radiation gets directly to space and a net power balance of 152 W/m^2—as expected from (2)—gets permanently recycled as part of the backscattered radiation.

For more appropriate multilayered atmospheres, we can take over the picture from the American Chemical Society (Figure 4).

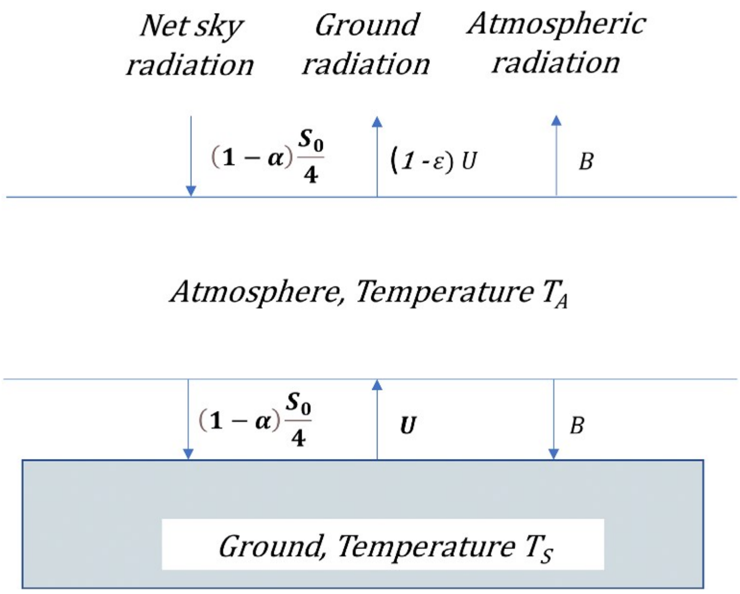

Figure 3. A single-layer model of the atmosphere, where S is the Solar irradiance, α is the cloud albedo and β the surface absorbance. U is the terrestrial radiation, of which a fraction $(1-\varepsilon)$ penetrates directly through the atmosphere to space and B is the radiation emitted by the atmosphere [5].

Instead of using layered-atmosphere models, there exist excellent semiempirical formulas to be used. Night skies are shielded by clouds and humidity against radiation loss, while clear and dry conditions cannot compensate for strong radiation losses. This has been studied e.g. with the modified Swinbank model [7] [8].

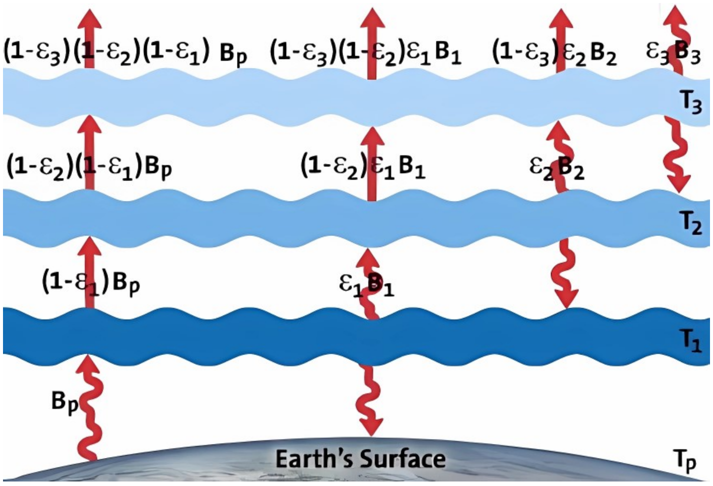

Figure 4. A multilayer atmosphere model illustrated here with three layers [6].

$$P_{SB} = \left(1 + KC^2\right) \cdot 8.78 \cdot 10^{-13} \cdot T_S^{5.852} \cdot RH^{0.07195} \quad (7)$$

with

P_{SB}	upwards and downwards directed atmospheric radiation in W/m²
K	0.34 clouds < 2 km, 0.18 for 2 km < altitude < 5 km, 0.06 for >5 km
C	Cloud cover (0 clear skies, 1 covered skies)
T	temperature in ˚K
RH	relative humidity in %

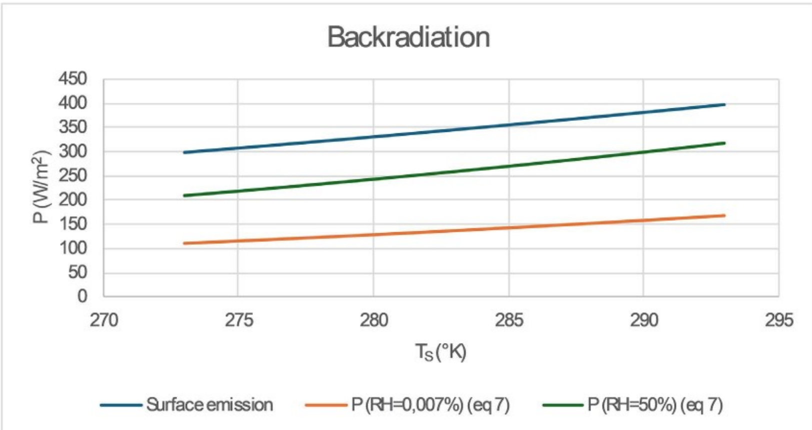

Figure 5. The effect of humidity on backward radiation compared between RH = 0.007% and RH = 50%. The blue line is the surface radiation at emissivity $\varepsilon_S \cong 0.95$ according to Stefan-Boltzmann.

As we can see in **Figure 5**, humidity has a strong impact and cloud coverage has even stronger impact on the back-radiation.

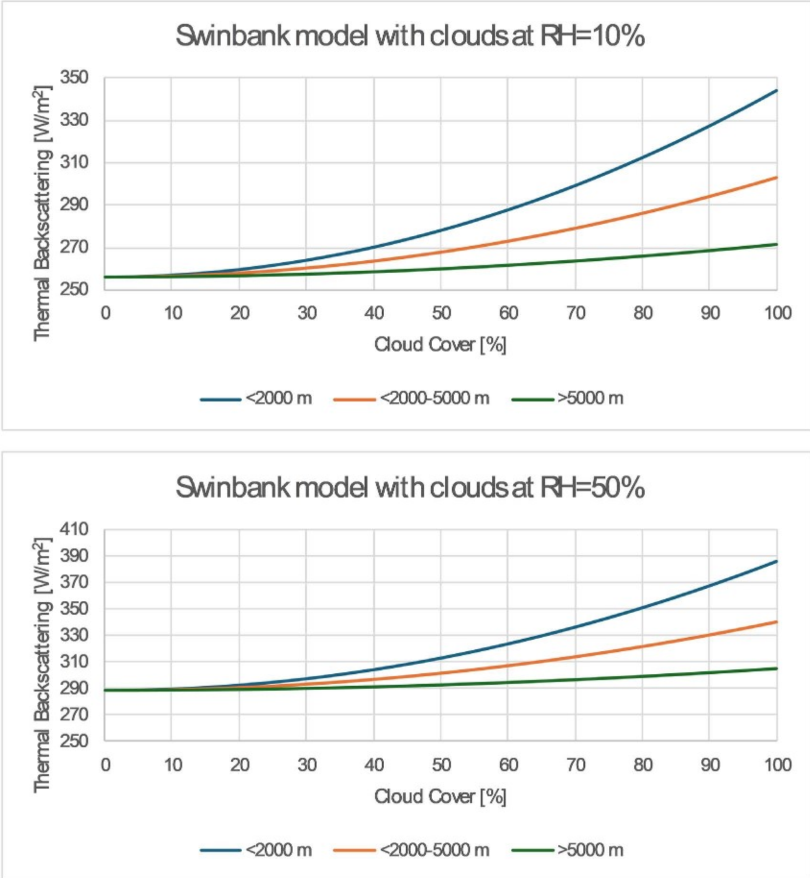

Figure 6. Thermal backward radiation characteristics of cloudy skies at RH = 10% and RH = 50%.

The last figures (**Figure 6**) suggest indeed that climate predictions depend critically on values like average relative humidity, cloud coverage, and albedo. These values vary considerably over the surface, depending on local temperature and geographic details. Gridded models can account for such values over years of observations to a certain extent only. Instabilities and risks due to erroneous positive feedback loop modeling and/or negligence of external geo-or astrophysical influences are obvious.

Data from ground measurements (**Figure 7**) indicate that the downward (backward) radiation of the atmosphere shows indeed full saturation of the IR CO_2 bands and does not support noticeable additional Thermal Forcing (TF) by increasing CO_2 in the lower atmosphere. It shows almost complete saturation of the 15 μ-central peak and close-to-saturation of the surrounding 15 μ band edges. Early studies [10] concluded as well that TF will not be significantly influenced by a further increase of atmospheric CO_2 (**Figure 8**). On the other hand, it is well known that concentrations below 50% of the current level would be detrimental to plant growth and climate.

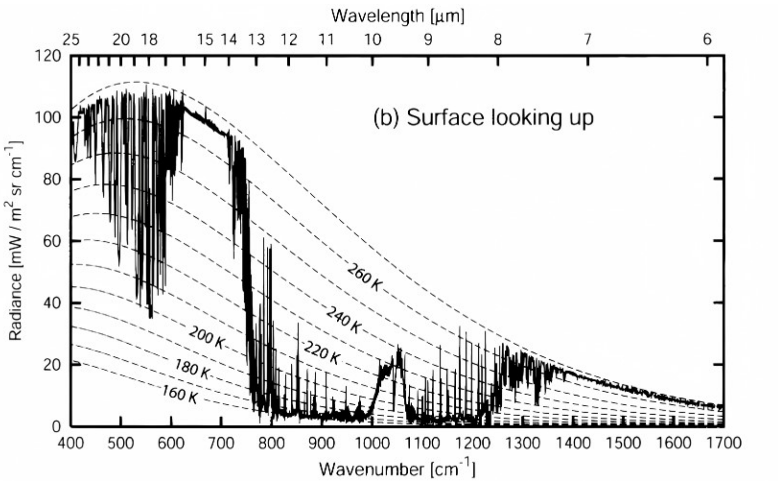

Figure 7. Measurements [9] of the infrared emission spectrum of the cloud-free atmosphere at the arctic surface looking upward.

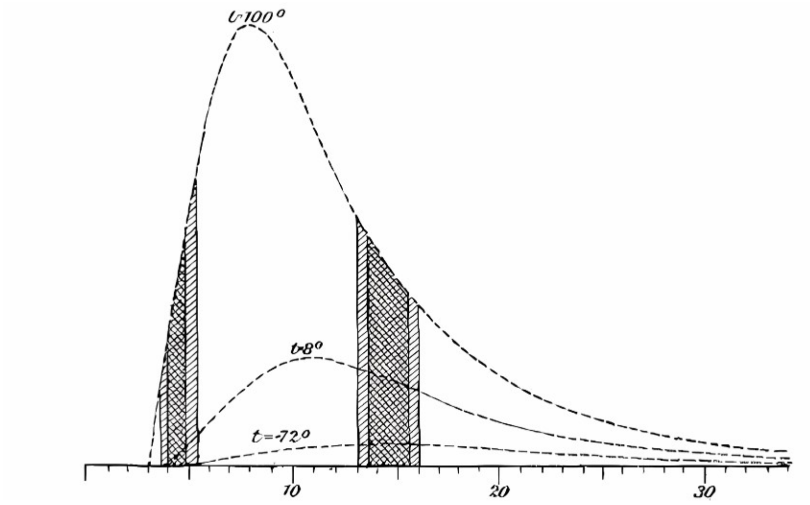

Figure 8. Studies of J. Koch at the Physical Department of Knut Angström [10].

The wavelength-dependent absorption a_λ and re-emission is calculated from Beers Law, where transmission is exponentially reduced by increasing absorber thickness L

$$a_\lambda(L) = 1 - t_\lambda(L) = 1 - \frac{I_\lambda(L)}{I_\lambda(0)} = 1 - e^{-k(\lambda, L)} \tag{8}$$

Kirchhoff's law requires that absorbed radiation should get emitted again, or in other terms absorptivity should equal emissivity. For a limited wavelength window, $\Delta\lambda$ the specific emissivity $\varepsilon_{\Delta\lambda}(L)$ is therefore obtained by

$$\varepsilon_{\Delta\lambda}(L) = \frac{\int_{\lambda_1}^{\lambda_2} I_\lambda(0) \cdot a_\lambda(L) d\lambda}{\int_0^\infty I_\lambda(0) d\lambda} \tag{9}$$

where the spectral extinction coefficient a_λ is obtained from HITRAN or similar databases.

The significance of the unsaturated edges in 15 μ band is highly overestimated, as it can be easily shown that with an extinction < 3 they contribute only 0.17% to the full band when we consider their respective integrals (Figure 9). This has also been shown by Howard [11] used further in this study.

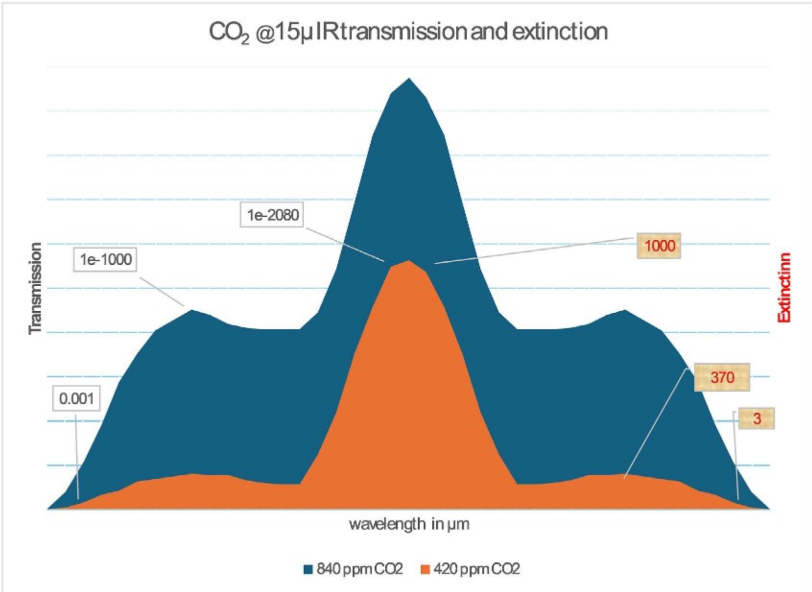

Figure 9. Transmission and Extinction Ratios in the 15 μ band.

The infrared (IR) spectra of the four main GH gases over a path length of 100 meters are presented in Figure 10, their concentrations being those that pertain to the atmosphere at sea level at 45% relative humidity.

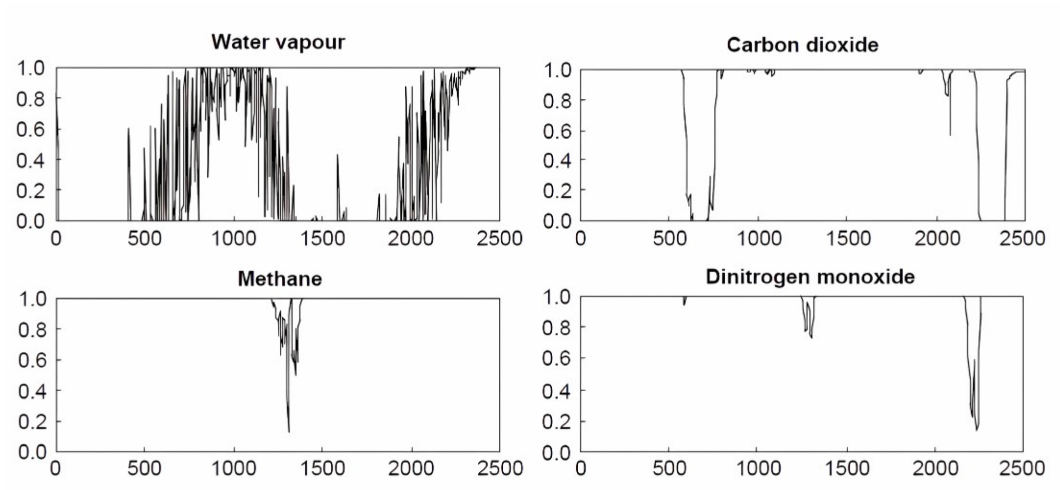

Figure 10. Infrared spectra of the main greenhouse gases as calculated using the HITRAN database; transmission is plotted against wavenumber (cm^{-1}) [4].

The 0 - 500 cm^{-1} band of H_2O at 45% RH absorbs 66% of the surface IR radiation. The 1300 - 1800 cm^{-1} band absorbs another 1%.

A 1 bar pressure atmosphere would have a theoretical thickness of 8.2 km. To visualize the effective column height of current CO_2 at different altitudes, we get the following Table 1.

Table 1. Equivalent of 400 ppm atmospheric CO_2 in meters at 1 bar atmospheric pressure.

H [m]	M(z)/M	1-M(z)/M	$L_{CO_2}^{up}$ [cm]	$L_{CO_2}^{down}$ [cm]
0	0	1	344.83	0.00
500	0.06893722	0.93106278	321.06	23.77
1000	0.1331221	0.8668779	298.93	45.90
5000	0.51045834	0.48954166	168.81	176.02
10,000	0.76034896	0.23965104	82.64	262.19
20,000	0.94256738	0.05743262	19.80	325.03
30,000	0.98623621	0.01376379	4.75	340.08
40,000	0.99670149	0.00329851	1.14	343.69
¥	1	0	0.00	344.83

where we obtained the altitude-dependent mass M from the barometric formula

$$\frac{M[z]}{M} = 1 - e^{-\frac{z}{H}} \tag{10}$$

with $H = 7$ km. The total mass below the altitude z is calculated as

$$M(z) = \int_0^z \rho(z')\,dz' = \rho(0)H\left(1 - e^{-\frac{z}{H}}\right) \tag{11}$$

The thickness of the CO_2-layer L_{CO_2} is a calculated value for a standard atmosphere at 1013.25 hPa and a total weight of 5.13 × 10^{15} tons of 8.21 km air at current 400 ppm. The table helps to understand the order of magnitudes when studying the atmospheric greenhouse effects of CO_2. It also illustrates that 75% of the total CO_2 is contained within the troposphere below 10 km altitude and 95% is below 20 km. If we were to concentrate all the CO_2 (at 400 ppm) of an 8.2 km thick atmosphere with a pressure of 1 bar in a single column, the height of the column would be around 3.5 m. The optical path length of CO_2 IR radiation at these conditions is below 1 cm and therefore we can expect full saturation already at current concentrations.

From thermodynamics we get

$$\frac{dT}{dz} = \frac{\gamma - 1}{\gamma} mg \Big/ R \tag{12}$$

where $\gamma = \frac{c_P}{c_v}$ (e.g. 7/5 for dry air), m = 29 g/mol and R is the gas constant. For the International Standard Atmosphere with $\gamma = 1.26$ we obtain $\frac{dT}{dz} = -6.5\,\mathrm{dK/km}$. Using this formula, we can estimate the LW back-radiation at higher altitudes (Figure 11), when substituting the $T_s \to T_s - \frac{dT}{dz} \times \Delta z$.

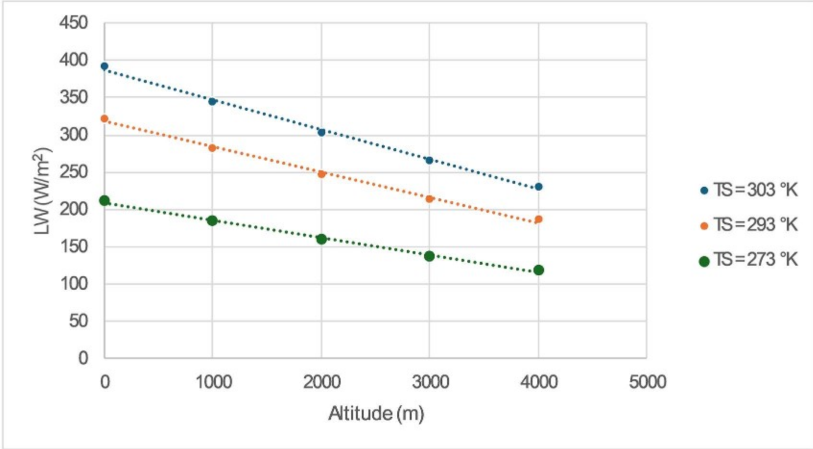

Figure 11. Estimated back-radiation in a standard atmosphere at three different surface temperatures.

This might be compared to measurements taken by a group from ETH Zurich in 1998 (**Figure 12**).

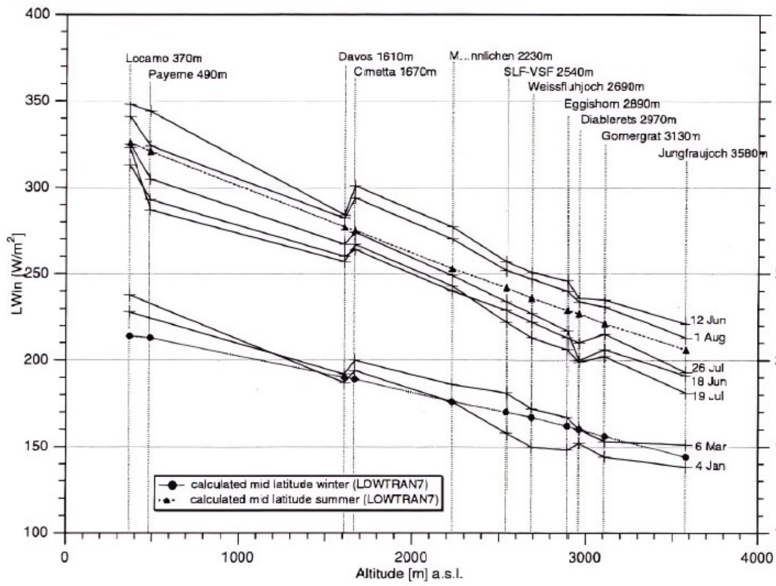

Figure 12. Altitude dependence of back-radiation with courtesy from C. Fröhlich [12].

The absorptivity *a* can be calculated using Beer's law for an infrared radiator from Equation (8) in a more generalized form.

$$a(c,L) = 1 - t(c,L) = 1 - \frac{I(c,L)}{I(c,0)} = 1 - e^{-k.c.L} \tag{13}$$

From Akram [13] we can obtain $k = 1.82 \times 10^{-6}\ \text{ppm}^{-1}\text{cm}^{-1}$ to calculate *a* as a function of *L*.

Figure 13 shows IR absorption saturation at current CO_2 levels already at air column length below 20 m. From this simple model, we must conclude that mechanisms other than CO_2 increases must explain significant atmospheric thermal enhancement (ATE) in the total energy budget.

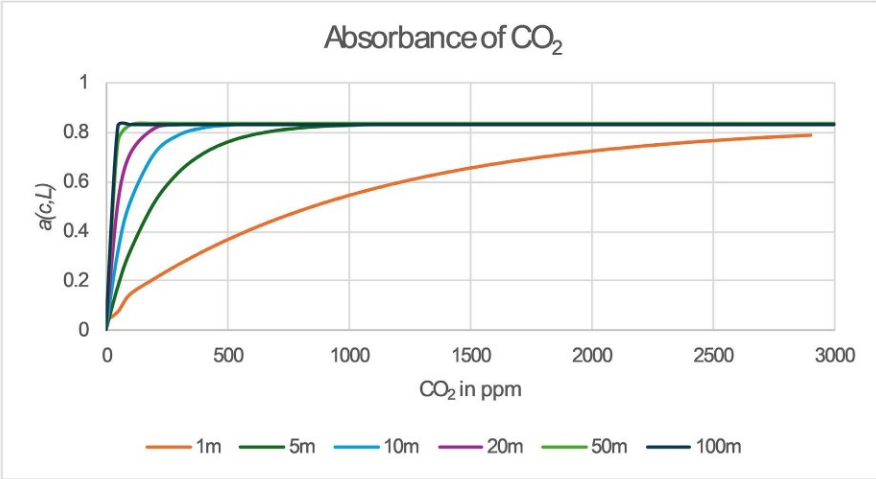

Figure 13. Absorbance of EMIRS200 IR light source in CO_2 from [13].

Howards [11] parameterizes the total absorption of strong lines at 15 μm and 4.3 μm according to

$$\int A_\nu d\nu = C + D\log w + K\log(p+P) \tag{14}$$

and

$$\bar{A} = \frac{\int A_\nu d\nu}{\nu_2 - \nu_1} \tag{15}$$

Substituting these values for $\nu_2 - \nu_1 = 250\text{cm}^{-1}$ in the 15 μm band and $\nu_2 - \nu_1 = 340\text{cm}^{-1}$ for the 4.3 μm band we obtain for a standard atmospheric layer of 1 km thickness (**Figure 14**) and for an 8.2 km thick atmosphere (**Figure 15**) as used for **Table 2**.

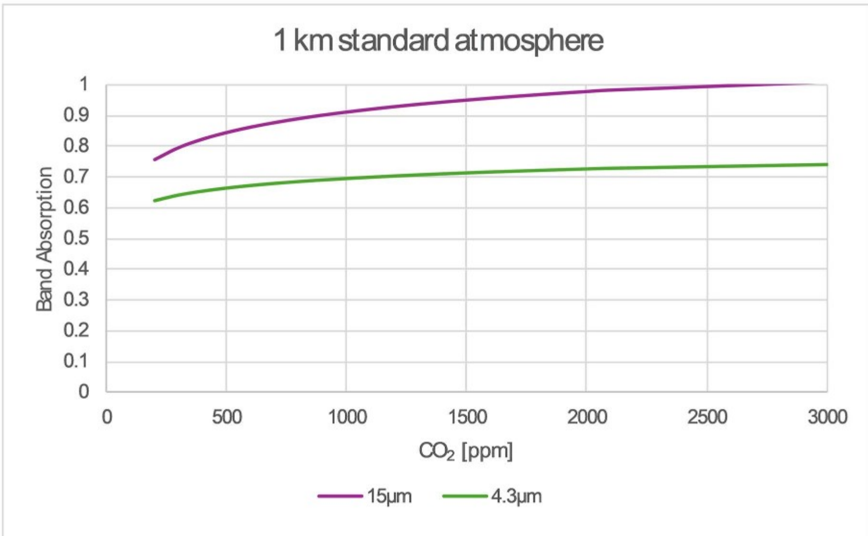

Figure 14. Band absorption within 1 km standard atmosphere [11].